CONSTRUCTION AND TESTING OF SMALL-SCALE THERMOACOUSTIC ELECTRICITY GENERATOR WITH DIFFERENT HEATING POWER

Ikhsan SETIAWAN[1], Irna FARIKHAH[2*], Anggi RAHMAWATI[1]

[1]Department of Physics, Faculty of Natural Sciences and Mathematics, Universitas Gadjah Mada, Indonesia

[*2]Department of Mechanical Engineering, Faculty of Engineering and Informatics, Universitas PGRI Semarang, Indonesia

[*]Corresponding author e-mail: irnafarikhah@upgris.ac.id

The necessity of renewable energy is indispensable. Nowadays, researchers focus on converting waste or solar heat into advantageous energy, such as electric energy, using thermoacoustic scientific knowledge. The thermoacoustic machine converts the heat energy into sound energy and conversely. Then, using a Linear alternator, it converts into electric energy. In this study, we focus on the construction and testing of small-scale thermoacoustic electricity generators with different heating temperatures. The heat is converted into acoustic energy employing the thermoacoustic engine, and the acoustic energy is converted into electrical energy using the linear alternator. In this investigation, the heating power varies from 226 W to 389 W. The result shows that 32.2 mW of electricity was found as the thermal power at 389 W. Moreover, the onset heating temperature span is 316℃.

*Keywords**: Thermoacoustic, engine, electricity, heating power*

1. Introduction

Energy consumption has rapidly increased due to technology development, rising population, and economic development [1]. These issues lead to the energy crisis in which the global demand on the limited natural mineral deposits used to power manufacturing companies and households is decreasing as the demand increases [2]. On the other hand, waste heat has become another environmental issue. Waste heat is often dissipated into the atmosphere or water like lakes, rivers, and the ocean. This increases greenhouse gas emission and contribute more to global warming [3]. The aforementioned issues can be solved using thermoacoustic technology. The waste heat can be transformed into sound energy, which can be used to drive the linear alternator to generate the electrical energy. Therefore, using thermoacoustic technology is good for the environment and renewable energy, especially electrical energy. Compared with the other technology, the thermoacoustic engine is pistonless so it will be easier and more applicable. Moreover, the improvement and accessibility of thermoacoustic refrigerators make them more effective and efficient than vapour compression refrigeration systems [4].

Thermoacoustic studies the interconnection between sound and heat with fluid and plate [5] and studies the transformation of heat to acoustic energy and conversely. Thermoacoustic can be divided

into two types: thermoacoustic engine and thermoacoustic cooler. The thermoacoustic engine is a machine for converting thermal energy into acoustic energy [6]. Then, the acoustic energy can generate electric power using a linear alternator or turbine.

The thermoacoustic engine has been investigated by some researchers. Ueda and Farikhah, in 2016, investigated the thermoacoustic energy conversion in the stack screen [7]. They proposed a thermoacoustic numerical calculation method incorporating the empirical formula for the laminated wire mesh regenerator proposed by Obayashi [8]. Using this method, the efficiency of energy conversion was numerically calculated in the laminated wire mesh regenerator of the thermoacoustic engine. The numerical results agree with the experimental results with an error of about 10%.

Furthermore, by comparing the energy conversion efficiency of the laminated wire mesh regenerator and the energy conversion efficiency of the regenerator with a uniform flow path, the effect of the complexity of the flow path on the efficiency can be clarified. Specifically, when the acoustic impedance is relatively low, and the temperature at the hot end is low, the flow path's complexity reduces the efficiency by nearly 40% [7]. This stack screen is usually used for the thermoacoustic engine. Other researchers focus on the effect of geometry on the efficiency of thermoacoustic [9-12]. Utami *et al.* did the numerical simulation and found that the lowest heating temperature to generate spontaneous oscillation in the thermoacoustic engine is 124℃ when the narrow channel radius of the stack is 0.12 mm. The temperature is the low-grade energy that can be utilized for waste heat recovery.

Moreover, the highest efficiency achieved as the flow channel radius stack equals 0.07mm. Thus, the efficiency is 57% of the upper limit value [9]. In 2020, Rokhmawati *et. al.* obtained the lowest initial heating temperature (153℃) and optimal efficiency (38 %) when the narrow radius of the engine stack is 5 cm and the mean pressure is 4 MPa [10]. The effect of the regenerator length on the performance of the prime mover system was numerically studied. It was calculated numerically that the engine efficiency is 27 % of the Carnot efficiency when the regenerator length corresponded to 6 cm [11]. Farikhah *et al.* designed a 4-stage engine for waste heat recovery to find the best radii of the 4-stage thermoacoustic engine and obtain the low temperature for the engine. It was found that the low onset heating temperature is 43℃, and the total system performance is 8% of the upper limit value when all of the ratio of narrow engine radii to the thermal penetration depth is 1.2 [12]. Farikhah et.al constructed the thermoacoustic cooler driven by a loudspeaker in 2013. Stem of goose down as an organic stack, a high thermal insulation material, was used for the plate media in the thermoacoustic engine. The goose down stack material has high thermal insulation, meaning it has low thermal conductivity of the plate media. There is no hazardous substance in the process, and piston is less. Air was used for the working gas, and stainless steel was used for the resonator. The decreasing cooling temperature is only 5℃ [13]. This cooler can be driven by the thermoacoustic engine. Some researchers optimized the performance by changing some geometries. It was found that the performance was improved by some optimized parameters [14-18]. The influence of the stack's porosity on the performance of a thermoacoustic refrigerator driven by a thermoacoustic engine was conducted. The best porosity of the engine and cooler is 1.1, and the entire performance is 24 % of the Carnot efficiency [14]. Liu *et al.* did the numerical calculation on a thermoacoustic refrigerator. They found that the larger the column number of staggered parallel plates, the better the refrigeration effect will be obtained [15]. Hakim *et al.* studied the potential of electric power generation using mechanic vibration; however, the electric power is still low [19].

The challenge of the thermoacoustic is the advancement of thermoacoustic electric generators. The thermoacoustic electric generator is a combination between a thermoacoustic engine and an alternator-like loudspeaker which operates in reverse mode. It transforms heat energy into acoustic work and then into electric energy. Nowadays, the investigations on traveling wave type of thermoacoustic electricity generator have attracted some researchers due to their better efficiency but with a more complicated configuration. Therefore, in this research, we focus on the standing wave type of thermoacoustic electricity generator due to its simplicity. In 2023, Ding and his group investigated thermoacoustic refrigeration systems driven by waste heat of industrial buildings. The cooling temperature achieved -12℃, and the cooling capacity is 0.95 kW. However, the configuration is more sophisticated [20].

In 2016 and 2019, Setiawan *et al.* investigated a thermoacoustic prime mover, but it did not apply to thermoacoustic electric power generation [21-23]. Kitadani *et al.* [24] constructed the traveling-wave and standing-wave type thermoacoustic electricity generator employing a Linear alternator to transform sound power to electricity and reach an electric power output of 1.1 W with a conversion efficiency from heat to electricity of 0.3 %. Piccolo [25] studied a numerical simulation of thermoacoustic electric power employing a conventional linear alternator in a straight tube. The study results show that the acoustic-to-electric performance is about 70 % when the heating temperature is 527℃, whereas the thermal-to-electric conversion efficiency generated by the prime mover is 5.7%. In 2022, Tutur *et al.* investigated pressure variation's influence on the initial temperature span and electric power output of a thermoacoustic electricity generator in a straight tube. It was found that the smallest onset heating temperature difference is 347℃ when the mean pressure is 0.35 MPa.

Moreover, 691 W of electrical power is achieved when the pressure is 0.40 MPa with 347℃ of onset temperature difference [26]. Moreover, the heating power used in this experiment is 370 W. In 2012, the traveling-wave thermoacoustic electricity generator using an ultra-compliant alternator was built and produced 11.6 W of electrical power. However, the device needed larger space, making the design more complex [27]. In 2014 Wang *et al.* performed the improvement of a 500 W thermoacoustic electric generator. They found a maximum electric power of 473.6 W at 2.48 MPa. It was found that the efficiency achieves 14.5 %, but the onset heating temperature is quite high at 650℃ [28]. A two-stage traveling-wave thermoacoustic electric generator was investigated. The study results show that 204 W of electric power is obtained, but the onset heating temperature is high at 597℃ and 511℃ [29]. The design and performance of a two-stage standing wave thermoacoustic electricity generator was investigated in 2016. Even though the electric power is high, the heating temperature of the engine is high [30]. Hamood and his group designed and constructed a two-stage thermoacoustic electricity; however, the mean pressure is too high [31]. A few researchers have investigated the influence of heating power on the onset heating temperature and electric power of a simple standing wave thermoacoustic generator. Therefore, we focus on it in this experimental study.

2. Experimental Method

The investigation was conducted using an experimental research approach. First, a standing wave thermoacoustic power with a branch was constructed. Then, some measurements were conducted, and the results related to the onset heating temperature difference, electric power, pressure, and frequency were presented.

2.1. Construction

The schematic diagram of the thermoacoustic electric power generation with the branch used in this investigation is illustrated in Fig.1. The system comprises some components: thermoacoustic engine core and Linear alternator. The thermoacoustic engine core is inserted into a pipe called a resonator. The resonator is made from stainless steel, and it is 29 cm in length. It is connected to the resonator branch, where the loudspeaker is located. The length of the connecting pipe is 16 cm, while the branch pipe is 24 cm in length. The other part of the resonator, made of polyvinyl chloride (PVC), has 36 cm in length.

In the engine core part, the stack, hot, and ambient heat exchangers are installed in the first part of the resonator. The stack is sandwiched by the hot and ambient heat exchangers. The length of the heat exchangers is 4 cm, whereas the length of the stack is 3.5 cm. The stack is made of a stainless-steel wire mesh screen with mesh number 12 [see Fig. 2 (c)]. The porosity of the stack φ is 0.814, while the wire diameter is 0.050 cm. Using the equation $r_{\mathrm{h}} \cong d_{wire}(\varphi/4(1-\varphi))$, the stack's hydraulic radius r_{h} is 0.0547 cm. This parameter shows the heat exchange process between the pore walls of the regenerator and the working fluid. δ_{k} is the thermal penetration depth, and τ is the thermal relaxation time in the cross-section of the regenerator's channel. The value δ_{k} is 2.0 defined as thermal penetration depth, which means the gas layer space in which heat can pour over an interval of time. It can be expressed as

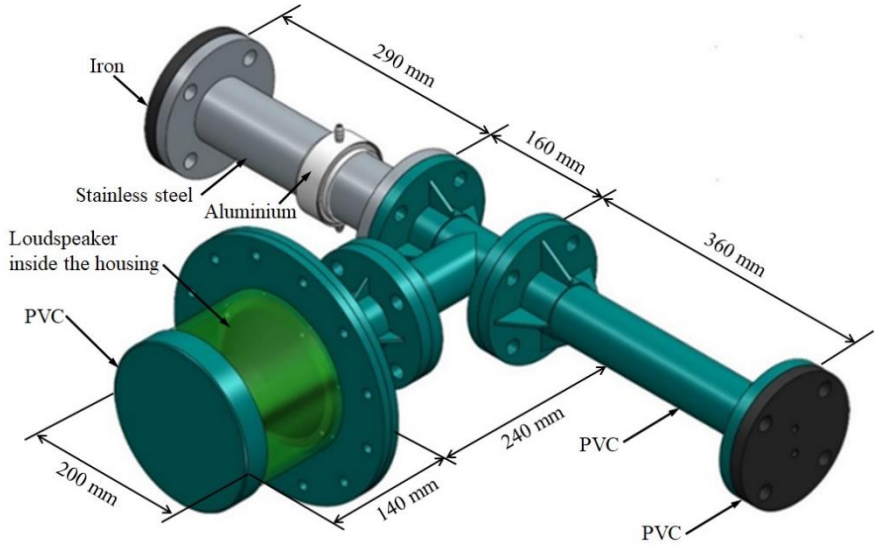

Figure 1. General design outline of a simple standing wave thermoacoustic electricity regenerator with branch

$$\delta_{\mathrm{k}} = \sqrt{k/\rho c_{\mathrm{p}} \pi f} \tag{1}$$

where k is thermal conductivity, ρ is density, c_{p} is the specific heat in the constant pressure, and f is the frequency. Those gas property values are shown in Table 1.

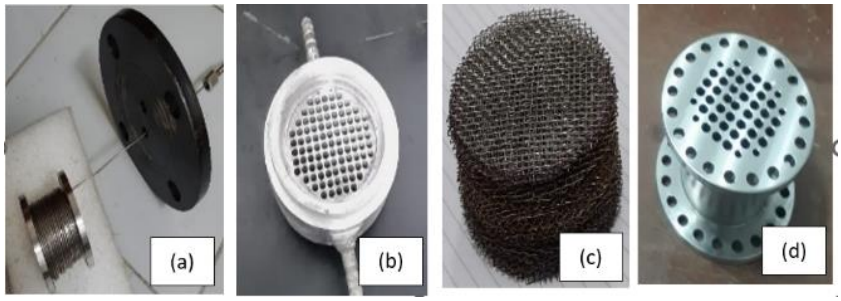

Figure 2. (a.) the heater (b.) the hot heat exchanger (c.) The screen mesh stack (d.) the ambient heat exchanger

The ambient and hot heat exchanger length are 4 cm, while the diameter is 6.8 cm. The heat exchangers have tiny holes with a diameter of 0.3 cm, and it is parallel to the axis of the resonator that allow the working fluid to oscillate to the pores. The heat exchangers are made of copper, which isa good thermal conductivity.

Fig. 2. (a) shows the heater used for heating the hot side of the stack. The hot and ambient heat exchangers are shown in Fig 2. (b) and (d). The heat exchangers have holes with a diameter of 0.3 cm, and it is parallel to the axis of the resonator, allowing the working fluid to vibrate to the tiny holes. The heat exchangers are made of copper, which is a good thermal conductivity.

Table 1. The module and T/S parameters of the loudspeaker

Specification		**Parameter "Thiele-Small"**	
Frame Diameter (Inch/mm)	6 inch / 15.24 cm	Resonance Frequency/Fs (Hz)	50 Hz
Impedance (**Ω**)	8 **Ω**	DCR (**Ω**)	5.0 **Ω**
Maximum Power (Watt)	60 W	Qts	0.78
Wide of frequency area (Hz)	50 Hz – 7.5 kHz	Qes	0.99
SPL (2.83 V/ 1m) (dB)	89 dB	Qms	3.59
Cone paper effective diameter (mm)	15.0 cm	Mms (g)	12.3 g
Magnetic Field (T)	1.15 T	Cms (mm/N)	0.078 cm/ N
Weight of Magnet (Kg/Oz)	0.27 kg/9.50 Oz	BL Product (Tm)	4.5 Tm
Voice Coil Diameter (mm)	2.54 cm	Vas (Liters)	20.4 Liters
Voice Coil material (mm)	Asv	No (%)	0.27 %
		Sd (**cm^2**)	136. 8 **cm^2**
IEC 268-5 (in box system, cut off 20-500 Hz)		Xmax (cm)	0.24 cm

The loudspeaker was employed as a linear alternator which converts acoustic into electric energy. It is located at the side branch, and it has 24 cm in length. The loudspeaker diameter is 15 cm, the impedance is 8 cap omega, and the loudspeaker terminals are connected to the resistor. The actual surface area of the loudspeaker cone is denoted as Sd, and it is 136.8 cm^2. The electrical power generated by the loudspeaker can be calculated using the following equation:

$$W_{\mathrm{e}} = \frac{V_{\mathrm{rms}}^2}{R_{\mathrm{L}}} \tag{2}$$

where W_{e} is the electric power, V_{rms} is the root mean square voltage, and the load resistance is denoted as R_{L}. The input electric power was turned on as the temperature at the stack hot side has not

elevated considerably. Therefore, the temperature span between the two sides of the stack remained constant. This system is assumed to be in a steady state condition. The temperature pressure amplitude and the electric voltage output are stopped after the electric power input is turned off. This step was repeated for heat input 226 W to 389 W.

The resonator used in the thermoacoustic engine part is 29 cm, while the connecting pipe is 16 cm. This pipe is connected to the other resonator, which is ,36 cm in length, and the side branch where the loudspeaker was placed. The total length of the resonator is 81 cm. The resonance frequency of the closed resonator tube can be calculated as follows:

$$f_{\mathrm{n}} = \mathrm{n}\, v/2L \tag{3}$$

where v is the speed of sound of the working fluid and L is the resonator length. The harmonic series frequency is denoted as f_{n}. n is n-th harmonic series (n = 1, 2, 3,…). By using the sound speed in Table 1 with a resonator length of 81 cm, the calculated resonant frequency with the heat input range of 226 W to 389 W is around 212 Hz for the first harmony frequency (n=1) and 424 Hz for the second harmony frequency (n=2).

Table 2. The gas properties [32]

P_{m}	0.1 MPa
γ	1.4
ρ_{m}	0.52 $\mathrm{kg/m^3}$
σ	0.707
C_{p}	1.0049 kJ/kgK
C_{v}	0.7178 kJ/kgK
c_{s}	348 m/s
K	0.026 W/(m·K)

Table 2 shows the gas properties determined at 0.1 MPa of mean pressure, and air was used as the working fluid (gas) at 300 K [32]. γ is the specific heat ratio, which is a dimensionless parameter $(C_{\mathrm{p}}/C_{\mathrm{v}})$. C_p and C_{v} are isobaric and isochoric specific heat, respectively. σ is the Prandtl number of the working gas, which is also a dimensionless number (ν/α). ν and α are kinematic viscosity and thermal diffusivity, respectively. P_{m}, ρ_{m}, c_{s}, and K are the mean pressure, density, sound speed, and thermal conductivity of the working fluid. The porosity shown in Table 3 is the dimensionless parameter, which is defined as the ratio of open area in the cross-section to the total cross section area of the stack.

Table 3. Length and Size

Total of the resonator length	81 cm
Length of stainless-steel resonator	29 cm
Length of connecting pipe	16 cm
Length of branch pipe	24 cm
Length of PVC Resonator	36 cm
Inner diameter of the pipe	5.5 cm
Length of stack	3.5 cm
Mesh number	12 strands/inch
Porosity of stack	0.814
Wire diameter	0.050 cm

Hydraulic radius	0.0547 cm
Length of ambient heat exchanger	4 .0 cm
Length of hot heat exchanger	6.8 cm
Diameter of small holes of heat exchanger	0.30 cm
Length of the linear alternator	2.4 cm
Diameter of the linear alternator	15.0 cm
Impedance	8.0 Ω

2.2. Measurement

To measure the temperature at the regenerator sides (T_{a} and T_{h}), the thermocouples were used. As the electric heater turns on, the thermocouples begin to record the temperature using the data logger. After the heat is imposed on the hot end of the regenerator, a spontaneous oscillation appears because of the temperature gradient on the thermoacoustic engine, and the sound wave is propagated. Then, the pressure versus time can be measured using the pressure sensors, displayed by a WE7000 data logger software. Using Fast Fourier Transform (FFT), the time domain data was transformed into the frequency domain. Four pressure sensors were used. To measure the oscillation pressure, the transducers are installed along the resonator tube. The pressure was measured using Kyowa PGMC-A-200 KP with nonlinearity and hysteresis within 1.34 % RO and 0.12 % RO, respectively. The temperature was measured using a type-K thermocouple with a special limit of error ± 1.1 K. The measurement error E_{m} is as follows:

$$E_{\mathrm{m}} = \sqrt{E_s^2 + E_r^2} \tag{4}$$

and

$$E_{\mathrm{r}} = \frac{\sqrt{\sum_{i=1}^{n} (y_i - \bar{y}_i)^2 / n - 1}}{\sqrt{n}} \tag{5}$$

where E_{r} is a random error, and E_{s} is a systematic error, n is the number of repeated measurements, and y_i is the arithmetic mean representing the y_{th} measurement [33]. Using eq. 4 and 5, the pressure and temperature measurement error can be estimated to be ± 4.00 Pa and ± 3.00 K, respectively.

To measure the heating power, the electric heater was introduced. It is imposed at the hot heat exchanger. At the ambient heat exchanger, the cooling water was circulated to maintain the ambient temperature. By using a digital voltmeter (measuring voltage V) and a digital ammeter (measuring current I), input heating power can be calculated as Q = VI (rms value).

In this investigation, the heating power was varied by the heater, and the acoustic power was generated inside the engine stack. Using some pressure sensors, the pressure can be measured, and acoustic power can be obtained. On the other hand, the temperature can be measured using and recorded in the data logger. The acoustic wave traveling is along the resonators and the side branch where the loudspeaker was located. In the loudspeaker, the acoustic energy was converted into the electric energy.

The prototype of a small-scale thermoacoustic electricity generator with a side branch configuration was built. Figure 4 shows the experimental setup. The system comprises a thermoacoustic engine, linear alternator, and resonator with branch. The engine regenerator is installed inside the resonator and is employed as the thermoacoustic engine. A loudspeaker was used for the

Linear alternator to transform acoustic into electric power. In this investigation, the atmospheric pressure was used. The working fluid is air, and the heat power is input into the system. The ambient heat exchange is running on the tap water and is using a water tank; the rejected water is collected. The temperature in the hot and ambient side of the engine regenerator was measured by the type E thermocouples, and the pressure transducers were obtained using data acquisition. It is connected to a data logger system. A power analyzer was employed to measure the current and voltage.

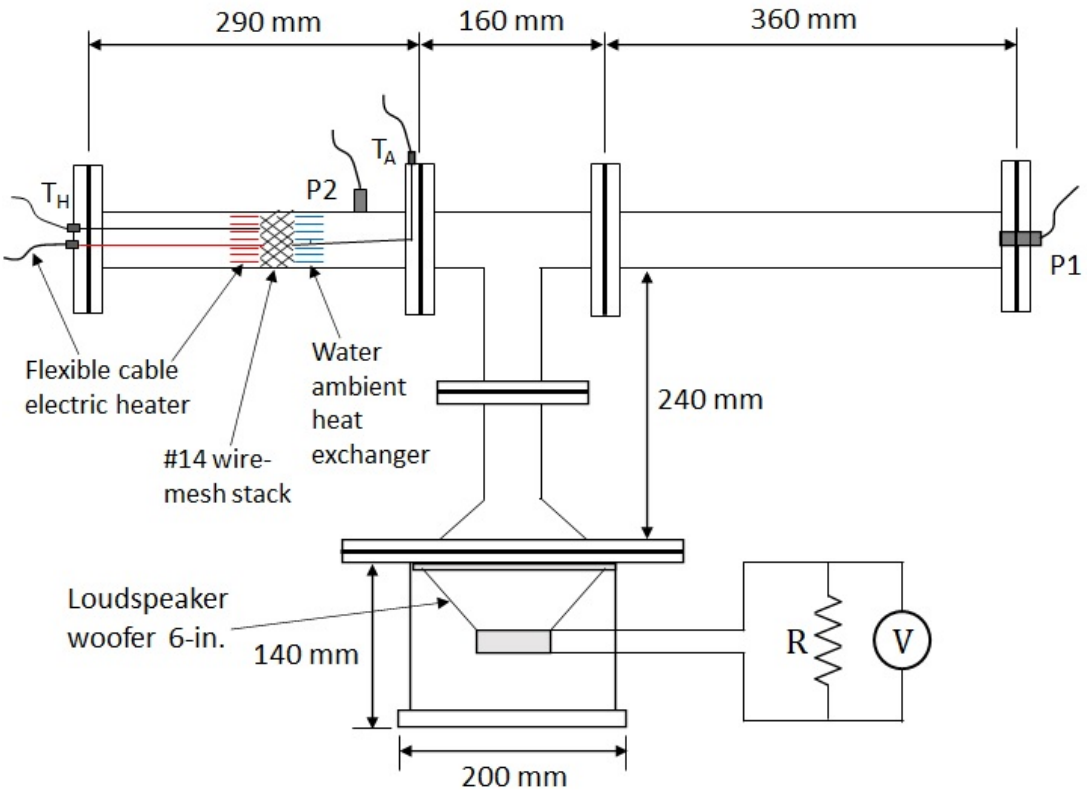

Figure 3. Experimental Setup of the thermoacoustic electricity generator with side branch configuration

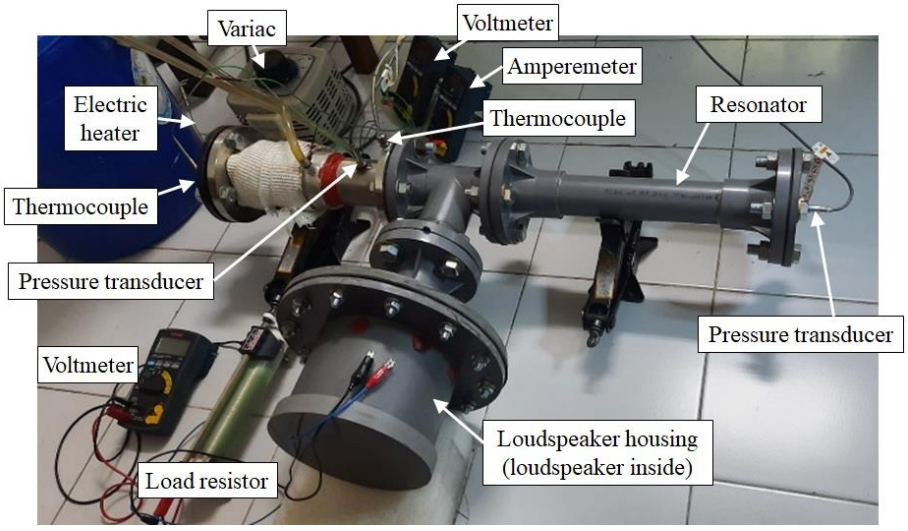

Figure 4. General arrangement of thermoacoustic electricity generator with side branch configuration.

3. Working Principle

Thermoacoustic electricity generator with side branch configuration comprises a resonator, a regenerator engine, a hot heat exchanger, an ambient heat exchanger, and a loudspeaker for the Linear alternator (See Fig. 3). The regenerator was arranged from the stack wire meshes in which the thermoacoustic effect occurs. The regenerator and the heat exchangers were installed in the resonator. In the thermoacoustic engine, there are no moving parts to perform the thermodynamics cycle. The presence of the regenerator plate and the working fluid is essential for the engine. When the heat source imposes the engine regenerator, the gas particles on one side become hot. As shown in Fig. 5, the gas particles experience four-step cycle: two constant pressure heat transfers in steps 2 and 4 and two adiabatic in steps 1 and 3.

Step 1 shows that the gas parcel experiences adiabatic compression while it displaces from the ambient side to the hot side. The fluid parcel is warmed. Then, in step 2, it experiences the constant-pressure heat transfer from the plate to the gas parcel. After that, the gas parcel in step 3 experiences adiabatic expansion, and it displaces from the hot side to the ambient side. In step 4, the gas parcel experiences constant-pressure heat transfer from the parcel to the plate. In step 2, the gas parcel experiences thermal expansion at high pressure, while in step 4, it experiences thermal contraction. As a result, the acoustic work is generated, $dW - dW'$. In this case, the acoustic energy is generated in the engine regenerator [6]. The acoustic power generated in the thermoacoustic engine is delivered into the loudspeaker where the conversion of the acoustic power to the acoustic power occurs.

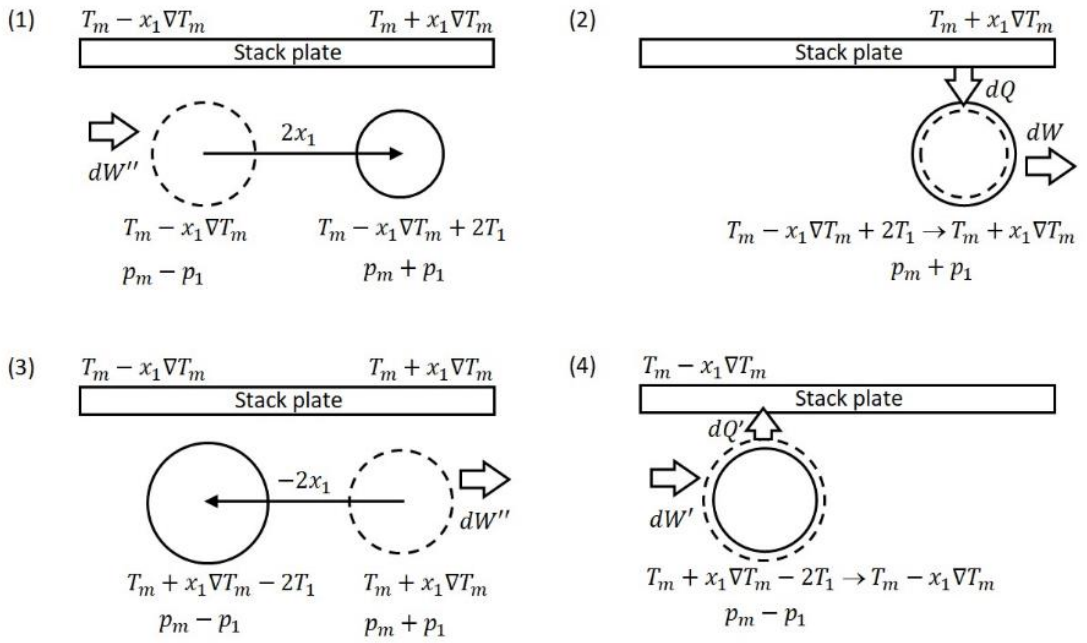

Figure 5. Typical fluid parcels occur in the stack [34]

4. Result and Discussion

Figure 6.a presents the result of measuring temperature as a function of time. This investigation used 0.1 MPa of air for the working gas. The red line shows the stack's hot side temperature, while the blue line presents the stack's ambient end temperature. Figure 6 shows that as the heater was turned on, the stack hot temperature rose considerably. On the other hand, the stack ambient temperature

remained constant. The spontaneous oscillation was excited when the onset heating temperature achieved a value. Then, the stack generated acoustic power. Figure 6.a shows the thermocouple's readings throughout experiment, which took 60 minutes. A 219 Hz was the spontaneous oscillation at the onset heating temperature T_h (344℃) with 28℃ of ambient temperature T_a. When the frequency is 219 Hz, the spontaneous oscillation occurs at the onset heating temperature T_h (344℃) with 28℃ of ambient temperature T_a. As a result, the onset heating temperature difference is 316℃. Thermal energy was converted to acoustic energy. Meanwhile, the linear alternator produced about 33 mW of electric power.

The pressure transducer is installed along the resonator tube. The pressure oscillation was measured using a transducer. Then, employing FFT, the frequency of the sound waves can be generated. Figure 6.b presents the frequency spectrum of the sound waves at 1 atm. It was taken at resonant frequency. As we can see in Fig. 6.b., the FFT analysis shows a dominant frequency of 219 Hz.

Figure 7 shows that the temperature difference occurs influenced by the heating power (besides being influenced by many factors). It can be seen that the onset temperature difference increases by approximately 2℃ from 314 to 316℃ when the heating power increases by 163 W from 226 W to 389 W. This happens because the temperature increases on the hot side of the stack becomes faster when the heating power is greater. The onset heating temperature difference is 316℃. Compared to that found by Tutur et al., this temperature is lower. They found 347℃, which means 31℃ higher than that found in this investigation [26]. One important thing is that the lowest heating power at 226 W, shown in Figure 7, is the minimum heating power needed so that the onset (thermoacoustic effect/sound generation) can occur. Heating power below 226 W cannot generate sound.

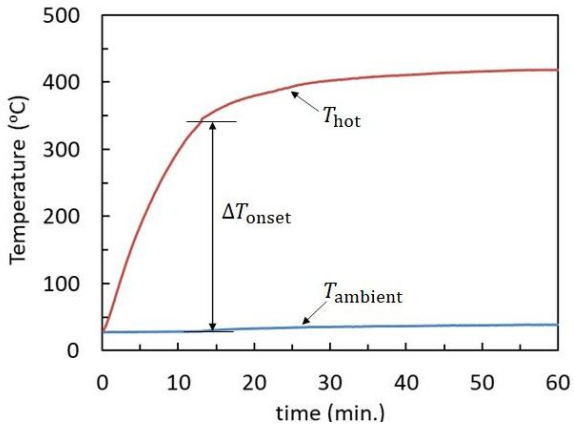

Figure 6.a. Temperature vs time over the testing period (60 minutes)

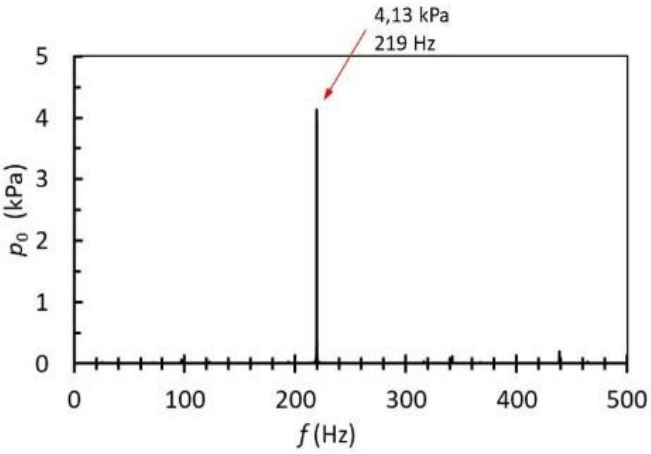

Figure 6.b. p_0 vs f

Heating power as a function of onset temperature difference ΔT_{onset} is shown in Fig. 7. When the heating power increases, the onset heating temperature difference rises from 314 to 316℃. Figure 8.a shows the experimental result of the frequency produced by the engine with different heating temperatures. It can be seen that the frequency slightly increases when the heat input increases. Figure 8.b shows the effect of heating power on the pressure amplitude p_1. It shows that the pressure amplitude increases from 2 to 5 kPa. The electric power generated by the loudspeaker in the steady

state is shown in Fig. 9. When the heat input is 226 W, the electric power is 8 mW, but when the heat input is 389 W, the electric power is about 33 mW.

Air is the working fluid at 100 kPa. r_h/δ_k has been calculated to be around 2.0. It means that thermal interaction between the working gas and the stack occurs effectively when the hydraulic radius of the pores of the stack is 2.0. The increase in ΔT_{onset} is the reason for the increase in frequency (f), pressure amplitude (p_1), and output electrical power (W_e).

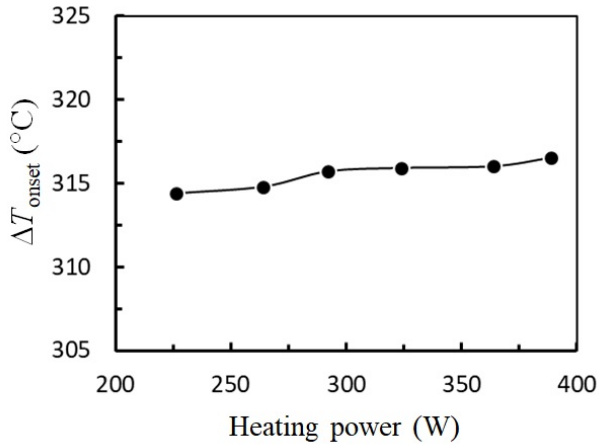

Figure 7. Heating power vs ΔT_{onset}

Figure 8.a shows that the frequency of the sound generated experiences a significant increase as the heating power increases. It increases by around 2.1 Hz, from 217.7 Hz to 219.6 Hz when the heating power increases from 226 W to 389 W. The increase in frequency occurs due to the increase in the maximum temperature difference, which comes from the increase in the temperature of the hot side of the stack (T_h). When the temperature T_h gets higher, the speed of sound increases in the gas. As a result, the sound frequency increases because the frequency f is proportional to the sound speed.

Figure 8.b shows that the amplitude of the generated sound wave pressure p_1 increases significantly as the heating power rises. It increases by around 2.1 Hz, from 217.7 Hz to 219.6 Hz, when the heating power increases from 226 W to 389 W. That is, around 2.34 times, from 2.10 kPa to 4.93 kPa, along with the increase in heating power from 226 W to 389 W. Therefore, the sound generated becomes stronger. Thus, the pressure amplitude becomes high.

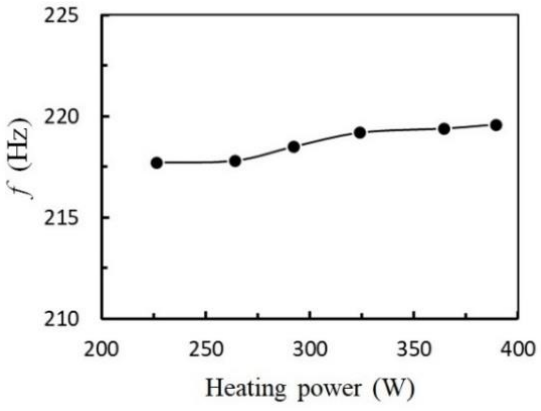

Figure 8.a Heating power vs f

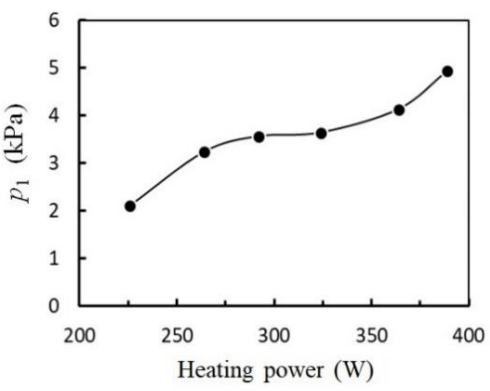

Figure 8.b. Heating power vs p_1

Figure 9 shows the dependence of the output electrical power produced by a thermoacoustic device on the heating power provided to the thermoacoustic device. It shows that the output electrical power increases almost linearly with the increase in heating power, with a very significant increase from 8.3 mW to 32.7 mW (about 4 times) when the heating power increases from 226 W to 389 W. The increase in output electrical power is caused by an increase in the onset temperature difference ΔT_{onset}, and pressure amplitude, which increases when heating power goes up. The electric power resulting in this investigation can be used for electronic applications, such as prescaler. This electronic device consumes 30 mW of electric power [35].

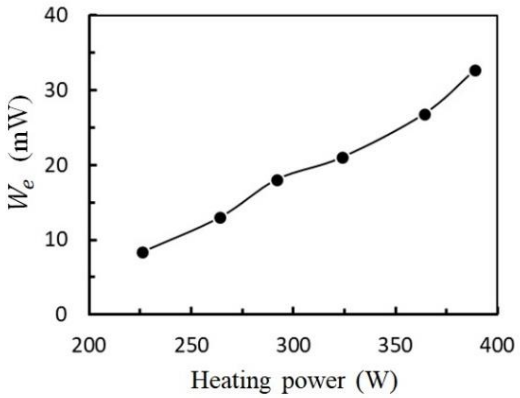

Figure 9. Heating power vs W_e

5. Conclusions

This study constructs a standing wave-type electricity generator with different heating power configurations. From the study results, the conclusions can be drawn as follows:

1) When the heating power is 389 W, the highest electric power can be achieved (33 mW). It can be seen clearly that the heating power has an impact on it. The higher heating power was achieved, the higher electric power would be obtained. The electric prower of 33 mW can be applied to electronic counting circuit, such as prescaler.
2) By changing the heating power, the difference in onset heating temperature increased, meaning that low heating power is preferable for low-grade waste heat recovery.
3) There is a trade-off between the dependence of electric power on heating power and those of onset heating temperature difference.
4) For low-grade waste heat recovery applications, the onset heating temperature difference and the electric power should be increased. Therefore, some parameters and working operation should be optimized for future work. Moreover, it is also essential that the geometry or the configuration of the thermoacoustic-electric generator should be investigated deeply to find the high electric power, best performance, and low heating temperature simultaneously.

Acknowledgment

The author would like to thank the Faculty of Mathematics and Natural Sciences, Universitas Gadjah Mada, for providing financial support through the 2023 Lecturer Research Grant Scheme with contract agreement number 14/UN1/FMIPA.1.3/KP/PT.01.03/2023.

References

[1] Dzioubinski, O., Chipman, R., *Trends in Consumption and Production: Household Energy Consumption*, United Nations, New York, USA, 1950.

[2] Ozili, P., Ozen, E., *Global energy crisis: impact on the global economy*, In Book: The Impact of Climate Change and Sustainability Standards on the Insurance Market, 2023.

[3] Bian, Q., Waste heat: the dominating root cause of current global warming, *Environmental System research*, 9 (2020), 8, pp. 2-11.

[4] Raut, A. S., *et. al*., Review of Investigations in Eco-Friendly Thermoacoustic Refrigeration System *THERMAL SCIENCE*, 21 (2017), 3, pp. 1335-1347.

[5] Tominaga, A., Thermodynamic aspects of thermoacoustic theory, *Cryogenic*, 35 (1995), 7, p. 427-440.

[6] Swift, G. W., *Thermoacoustics: A Unifying perspective for some engines and refrigerators*. Acoustical Society of America, New York, USA, 2002.

[7] Ueda, Y., and Farikhah, I., Calculation of energy conversion efficiency of a stack-screen Regenerator using thermoacoustic theory, *TEION KOGAKU (Journal of Cryogenics and Superconductivity Society of Japan)*, 51 (2016), 8, pp. 403-408.

[8] Obayashi, A., *et. al*., Amplitude Dependence of thermoacoustic properties of stacked wire meshes, *TEION KOGAKU*, 47 (2012), 9, pp. 562-567.

[9] Utami, S., *et. al*., Numerical study of the influence of radius regenerator on the low heating temperature and efficiency of travelling wave thermoacoustic engine, *J. Phys.: Conf. Ser*, 1464, (2020).

[10] Rokhmawati, E. D., *et. al.*, Numerical study on the effect of mean pressure and loop's radius to the onset temperature and efficiency of travelling wave thermoacoustic engine, *Automotive Experiences*, 3 (2020) pp. 96-103.

[11] Farikhah, I., *et. al*., Study of regenerator length on efficiency of thermoacoustic engine, *Proceedings*, the 3rd IEEE Eurasia conference on IOT, communication and engineering, Yunlin. Taiwan, 2021, pp. 580-582.

[12] Farikhah, I., *et. al.*, Numerical Study on the Effect of Regenerator Radii on the Low Onset Heating Temperature and Efficiency of 4-Stage Thermoacoustic Engine". *Arab J Sci Eng*, 48 (2022) pp. 2769-2778.

[13] Farikhah, I., *et. al.*, Thermoacoustic design using stem of goose down stack, *Proceedings, American Institute of Physics (AIP)*, 19th International Symposium on NonLinear Acoustic (ISNA 19). 1474, 2012, pp. 283-286.

[14] Farikhah, I., Ueda, Y., The effect of the porosity of regenerators on the performance of a heat-driven thermoacoustic cooler, *Proceedings*, The 24th International Conference on Sound and Vibration (24 ICSV) London, 2017.

[15] Liu, L., *et. al.*, Numerical Study on a Thermoacoustic Refrigerator with continuous and staggered arrangements, *THERMAL SCIENCE*, 26 (2022), 26, 5A, pp. 3939-3949

[16] Farikhah, I., Ueda, Y., Numerical calculation of the performance of a thermoacoustic system with engine and cooler regenerators in a looped tube, *Appl. Sci.*, 7 (2017), pp. 672.

[17] Farikhah, I., The effect of mean pressure on the performance of a single stage heat-driven thermoacoustic cooler, *Int. J. Low-Carbon Technol*. 15 (2020), pp. 471–476.

[18] Liu, L., *et. al.,* Dynamic Mesh Modeling and Optimization of a Thermoacoustic refrigerator using response surface methodology, *THERMAL SCIENCE,* 22 (2018), 2, pp. S739-S747.
[19] Hakim, M. A. D., *et. al.,* The Potential of Mechanic Vibration for Generating Electric Energy. *Advance Sustainable Science, Engineering and Technology (ASSET),* 2 (2020), pp. 0200206-01-06.
[20] Ding, X., *et. al.,* Zhuo Chen, Huifang Kang, Lingxiao Zhang, Research on thermoacoustic refrigeration system driven by waste heat of industrial buildings, *Sustainable Energy Technologies and Assessments*, 55 (2023).
[21] Setiawan, I., *et. al.*, Experimental Study on a Standing Wave Thermoacoustic Prime Mover with Air Working Gas at Various Pressures, *Journal of Physics*: Conference Series, 710, (2016), pp. 012031.
[22] Setiawan, I., *et. al.,* Influence of parameter on the performance of a standing-wave thermoacoustic prime mover, *Journal of Physics*: Conference Series, 1755 (2016), pp. 110004, January 2016.
[23] Setiawan, I., *et al.,* Traveling-wave thermoacoustic engine with pressurized air working gas**,** *Journal of Physics*: Conference Series, 2088 (2019), pp. 030022.
[24] Kitadani, Y., *et al.,* Basic study for practical use of thermoacoustic electric generation system, *Proceedings*, 20th International Congress on Acoustics, (2010), pp. 1-4.
[25] Piccolo, A., Study of Standing-Wave Thermoacoustic Electricity Generators, *Sustainable Energy Technologies and Assesments*, 26 (2018), pp.17-27.
[26] Tutur, U., *et. al.,* Influence of pressure variation of air working gas on the onset temperature difference and electric power output of a standing wave thermoacoustic electricity generator, AIP Conference Proceedings, 2391, 2022, pp. 090028.
[27] Yu, Z., *et. al.,* Travelling-wave thermoacoustic electricity generator using an ultra-compliant alternator for utilization of low-grade thermal energy, *Applied Energy*, 99 (2012), pp. 135-145.
[28] Wang, Kai., *et. al.,* Operating characteristics and performance improvements of a 500W traveling-wave thermoacoustic electric generator, *Applied Energy*,160 (2015), pp. 853-862.
[29] Kang, H., *et. al.,* A two-stage traveling-wave thermoacoustic electric generator with loudspeakers as alternators, *Applied Energy*,137 (2015) pp. 9-17.
[30] Piccolo, A., Design issues and performance analysis of a two-stage standing wave thermoacoustic electricity generator, *Sustainable Energy Technologies and Assessments*, 26 (2018), pp 17-27.
[31] Hamood, A., *et. al.,* Design and construction of a two-stage thermoacoustic electricity generator with push-pull linear alternator, *Energy*, 144 (2018), pp. 61-72
[32] Engineering ToolBox (2001) [online] Available at: https://www.engineeringtoolbox.com [Accessed 12 November 2023]
[33] Hsu, S-H., Lai, C-H., Evaluating the onset conditions of a thermoacoustic Stirling engine loaded with an audio loudspeaker. *Front. Front. Therm. Eng*., 3 (2023), pp.1241411
[34] Swift, G. W., Thermoacoustic engines, *J. Acoust. Soc. Am*, 84 (1988), pp.1145-1180.
[35] Knapp, H., *et. al.,* "2-GHz/2-mW and 12-GHz/30-mW dual-modulus prescalers in silicon bipolar technology," in *IEEE Journal of Solid-State Circuits*, vol. 36, no. 9, pp. 1420-1423, Sept. 2001, doi: 10.1109/4.944671

Submitted: 06.07.2023.
Revised: 20.12.2023.
Accepted: 28.12.2023.